Paper No.
11010

NACE INTERNATIONAL CORROSION 2011 CONFERENCE & EXPO

Cathodic Behavior of ~9% Cr Steel Reinforcement in Concrete

Mersedeh Akhoondan and Alberto A. Sagüés
Department of Civil and Environmental Engineering
University of South Florida
4202 East Fowler Ave.
Tampa, FL 33620 U.S.A.

ABSTRACT

The extent of the oxygen reduction reaction in concrete was evaluated for ~9% Cr rebar approaching the ASTM A1035 specification and compared to that of conventional carbon steel rebar, at ages of up to ~ 1year. Cathodic strength was measured by the cathodic current density developed at -0.35 and -0.40 V ($Cu/CuSO_4$) in cyclic cathodic potentiodynamic polarization tests, both in the as-received condition with mill scale, and with scale removed by glass bead surface blasting. In both conditions the ~9% Cr alloy was a substantially weaker cathode, by a factor of several fold, than carbon steel. Within each material, the surface blasted condition yielded also much lower cathodic current density than the as-received condition. These trends indicate an additional benefit in the application of ~9% Cr alloy as an alternative material to CS. There was strong correlation between the charge storage capability of the interface and the extent of cathodic reaction of oxygen. The result cannot be ascribed solely to differences in effective surface area between the different materials and conditions.

Key Words: 9% Cr, steel reinforcement, rebar, concrete, cathodic reaction, mill scale, glass bead blasting, corrosion

INTRODUCTION

The corrosion of reinforcing steel in highway structures costs the U.S. economy billions of dollars annually.[1] To achieve increasingly longer structural service life goals (e.g. >75 years), alternative corrosion-resistant reinforcing steel bar (rebar) materials merit consideration. Since chloride contamination above a threshold value C_T is a major cause of rebar corrosion, materials with higher C_T values are desirable. Those include stainless steels (containing > 12% Cr) which in a scale-free condition have well documented much higher C_T values than plain carbon steel (CS).[2] Recently, reinforcing steel with ~9% Cr (ASTM A1035)

has received increasing attention, as that alloy still has C_T > ~ several times that of CS but moderate added cost.[3] An added benefit of Cr- alloys beside their higher C_T value is that the oxygen reduction rate taking place on the passive surface of these materials, at a given potential, tends to be less than for CS. The effect is beneficial because the corrosion of steel in concrete after C_T is reached is often localized, and a major part of the cathodic reaction, oxygen reduction (Eq. 1) occurs on surrounding passive steel surfaces.

$$O_2 + 2H_2O + 4e^- \rightarrow 4OH^- \quad (1)$$

The rate of oxygen reduction reaction on passive surfaces away from the active anodes tends to control the corrosion rate at the anode [Figure 1] so a lesser ability to sustain cathodic reactions is desirable for alternative rebar materials. Previous work by Pedeferri et al [4] and others documented instances of significant lower cathodic corrosion rates in alloy steels in concrete or alkaline environments.[5] There is however indication that the presence of mill scale can lessen the cathodic differentiation between CS and stainless steels.[4,5] Little information is available on these issues for the case of the moderate Cr content steels including the 9% Cr alloy. The objective of this work is to investigate the cathodic performance of commercially available ~9% Cr reinforcement relative to that of conventional steel bars, with and without the presence of mill scale.

EXPERIMENTAL PROCEDURE

As-received (with mill scale) and surface blasted 16 mm diameter (No. 5) 9% Cr alloy rebars and 13 mm diameter (No.4) plain carbon steel rebars, with respective exposed areas of 70cm^2 and 56cm^2 [Figure 2] were placed in standard 15 cm diameter by 30 cm height concrete plastic molds. The 9% Cr steel nominally conformed to ASTM A 1035 and the carbon steel bars were produced per ASTM A 615. Metallographic examination and chemical composition analysis findings are presented in the Results Section. Surface blasting by glass beads (~200 μm diameter) using an ordinary sand blasting cabinet was performed, applying the air jet locally for about 2 seconds with moderate air pressure until bright metal was seen on the entire rebar surface. The concrete was made with 384kg/m^3 of Portland cement Type 2, w/c=0.5, limestone coarse aggregate (maximum diameter of 3/8-in) and silica sand. There was a total of 4 cells; each cell contained two rebars of different types and configured as shown in Figure 3, so all rebar conditions were tested in duplicate in different cells. After demolding following 5 days cure, the edges of rebar where it emerged from concrete were sealed with epoxy. Rebar potentials were measured against an internal embedded activated titanium electrode [6] that provided high interim stability. The internal electrode was periodically calibrated against an external Cu/$CuSO_4$ electrode (CSE) as detailed in the next section. All tests were performed at room temperature, keeping the concrete cylinders partially covered and with occasional surface rewetting to retard long term drying. Cyclic cathodic potentiodynamic polarization (starting at the open circuit potential (OCP), forward scan to ~ -500 mV and return scan back to the OCP) were conducted at a scan rate of 0.05 mV/sec. The calibrated internal reference electrode was used for all polarization measurements. An activated titanium mesh embedded near the top of the cylinder served as the counter electrode (Figure 3). Cyclic polarization tests were performed in groups conducted at various times over a one-year period after casting. Each group of tests spanned a period of up to 2 weeks centered on a nominal test group date. All potentials are reported on the CSE scale.

RESULTS AND DISCUSSION

Metallographic cross section analysis of carbon steel specimens showed typical hypoeutectoid microstructure, with fine pearlite (estimated carbon content ~0.6%). Scanning Electron Microscopy (SEM) images of the etched cross sections obtained at 12000X are shown in Figure 4. The Microstructure of the 9% Cr alloy was consistent with the reported combination of martensite laths with austenite between the laths.[7] Energy Dispersive Spectroscopy (EDS) of the cross sections, Table 1, confirmed the nominal 9% Cr content of the A 1035 rebar material used for this experiments as well as the expected major components in the CS rebar material. Figure 5 shows SEM views of the mill scale on the as-received 9% Cr and CS. The latter and seems rougher, but relative roughness may be different depending on the magnification used.

Figure 6 shows the OCP evolution for about one year following casting. Variations in the scan apex position reflect post-test correction of reference electrode potential per the procedure described later on. All alloys showed progressive ennoblement during the exposure, indicating slow maturing of the passive film. For both CS and 9% Cr potentials tended to be more negative in the surface blasted than in the as-received condition, suggesting less cathodic strength in the former. Representative cathodic polarization graphs for CS and 9%Cr are shown in Figure 7. The curves showed Tafel-like behavior and moderate hysteresis (greater for CS and the as-received conditions of both materials). The CS curves, especially in the as-received condition may show signs of mixed activation-concentration polarization behavior at the more negative potential values. Combined polarization curves were constructed using, for each potential, the average (i) of the forward- and reverse- scan currents (i_f, i_r). Those curves corresponded to typical apparent Tafel slopes of 150 mV for the 9% Cr (both surface blasted and as-received conditions) and 240 mV (as-received) and 140 mV (surface blasted) for the CS. Allowing for some concentration polarization, the results are roughly consistent with those expected for oxygen reduction on these materials.[8,9]

Cathodic performance was quantified by the value of i at -0.40 V_{CSE}, representative of typical polarization levels in concrete corrosion macrocells [9, 10], and at -0.35 V_{CSE} addressing a milder cathodic polarization level. Results for all specimen categories and test times are illustrated in Figures 8. There was variability in the results from duplicate specimens and with test time. However, while there was no well-defined trend in evolution of behavior with test time, clear differentiation existed in relative cathodic strength of different materials and surface conditions.

To examine those differences, the cathodic current densities obtained for each pair of specimens for a given material and condition were averaged at each test time, and the result averaged again over the ~1 year test period. Ratios between the resulting averages were then computed. Figure 9 shows that for both CS and 9% Cr the as-received surface condition resulted in a much stronger cathode than for the surface blasted condition, consistent with the open circuit potential trend noted above. The corresponding current density ratio ranged from about 2 ½ to 5. The ratio was comparable at the two evaluation potentials.

More relevant to the scope of this work, Figure 10 shows that for both the as-received and the surface blasted surface conditions CS was a substantially stronger cathode than 9% Cr, by a factor of about 4 at both evaluation potentials. It is noted that prior work with polished

cross sections of comparable alloys in simulated pore water solutions [8] also yielded much greater cathodic current densities for CS compared to 9%Cr. The cathodic current density ratio in that earlier work (~10) was found to be even greater than in the present case, but it remains to be determined whether that difference falls outside the range of uncertainty inherent to the present tests, some of which is discussed next.

It is noted that an important source of data scatter in these experiments was day-to-day (~50 mV) and long term (~150 mV) variability of the apparent OCP as measured by the CSE placed on the surface of the concrete. This type of scatter is not uncommon in concrete tests.[11] Some of that variability was reduced by using consistent pre-wetting of the concrete surface in a cavity normally covered by a stopper to prevent carbonation by atmospheric CO_2 at the test point. Additional compensation for long term drift was made by creating new cavities at age ~120 days and again ~220 days then interpolating accordingly with a smoothed function for the intervening measurements; the OCP values reported in Figure 6 were obtained after correction in that manner. The remaining uncertainty affects however the potential value chosen for determination of the cathodic current, with resulting random and systematic error. Relative trends tended to be less affected by this issue as the long term variations tended to be shared by all specimens. Thus, strong differentiations between materials and surface conditions such as those noted above are well established while recognizing that precise ratio determination remains elusive.

.

The forward/reverse hysteresis in the cathodic scans (Figure 7) may be speculatively interpreted as reflecting an interfacial charge storage phenomenon that is independent of the oxygen reduction reaction. The extent of hysteresis for each material and condition was quantified by a charge storage parameter (C_S), equal to the value of a hypothetical ideal interfacial capacitance that, at the scan rate (S_R) used and at a given potential, would have produced the same difference between i_f and i_r as observed experimentally. Following the treatment described elsewhere[9], the value of C_S can be calculated from the data by

$$C_S = 2\ S_R / (i_f - i_r) \qquad (2)$$

The results, averaged for each material and surface condition over the ~1 year test interval are shown in Figure 10. Figure 11 shows in a composite graph the average C_S values of individual specimens contrasted with the average values of i obtained for the same specimens at the same potentials. Notably, there was strong and nearly linear correlation between both quantities. The C_S values were about one (surface blasted condition) to two (as-received surfaces) orders of magnitude greater than those expected for typical double layer capacitances of smooth and clean metallic interfaces.[12] This is not surprising since charge storage in these systems is expected to be complicated by surface roughness, porosity, and formation/dissolution at near equilibrium condition of interfacial species [14] including reversible changes of oxidation state on the specimens with mill scale. Comparable apparent capacitance values are often reported from impedance measurements in concrete at frequencies low enough to be consistent with the cycling time of the potentiodynamic scans used here, and ascribed to similar causes.[13] Continuation work in this system with impedance measurements and an additional series of tests in concrete is in progress.

The correlation between i and C_S suggests that the factors responsible for greater charge storage capability also enhanced the rate of the cathodic reaction. One likely factor would be surface roughness or increased scale porosity, with consequent increased surface

area for reaction. The apparent greater roughness of the scale on CS compared to that of 9%Cr rebar, Figure 5, would favor that explanation for the materials in the as-received condition. However, relative roughness and porosity may be quite different at other size scales not easily revealed by microscopic examination. Relative roughness may not be a key factor either in accounting for the differentiation between both alloys in the scale free condition, since a high CS / 9% Cr cathodic current density ratio was also found in the previously cited study with equally finely polished surfaces.[8] Those differences may be best ascribed instead to the effect of the presence of Cr in the electronic properties of the passive film.[15] These issues are being considered in continuation work.

Regardless of the mechanism responsible for the difference, this investigation revealed a substantial reduction in cathodic strength in the 9% Cr alloy compared with CS in both the as-received and clean surface conditions. The beneficial impact of that decrease can be evaluated by incorporation in predictive models for the corrosion propagation rate of steel in concrete when corrosion macrocells are present.[9,16]

CONCLUSIONS

- The oxygen reduction cathodic current density at potentials of -0.35 and -0.40 V_{CSE} was chosen as the indicator of cathodic strength. Results for one year of exposure showed that in both the as-received and surface blasted conditions the ~9% Cr alloy was a substantially weaker cathode, by a factor of several fold, than carbon steel. Within each material, the surface blasted condition yielded also much lower cathodic current density than the as-received condition. These trends indicate an additional benefit in the application of ~9% Cr alloy as an alternative material to CS.

- There was strong correlation between the charge storage capability of the interface and the extent of cathodic reaction of oxygen. The result cannot be ascribed solely to differences in effective surface area between the different materials and conditions, and needs to be examined in terms of the electronic properties of the passive films and scales on the rebar surface in each condition.

ACKNOWLEDGEMENTS

The authors appreciate the assistance of the University of South Florida Nanomaterials & Nanomanufacturing Research Center and Mr. Joshua Schumacher and Mr. Paul Clark in performing experimental data acquisition, and of the Florida Department of Transportation in preparing and casting the concrete. The opinions, findings and conclusions expressed in this publication are those of the authors and not necessarily those of any of the assisting agencies.

REFERENCES

1. "Historic Congressional Study: Corrosion Costs and Preventative Strategies in the United States, a Supplement to Materials Performance", (Houston, TX: NACE, 2002).

2. M.F. Hurley, J.R. Scully, "Threshold Chloride Concentrations of Selected Corrosion Resistant Rebar Materials Compared to Carbon Steel", Corrosion Science, Vol. 62, No. 10, (Houston, TX, 2005).

3. F. Presuel-Moreno, J.R. Scully, S.R. Sharp, “Literature Review of Commercially Available Alloys That Have Potential as Low-Cost, Corrosion-Resistant Concrete Reinforcement”, Corrosion Science, Vol. 66, No. 8, (2009).

4. L. Bertolini, B. Elsener, P.Pedeferri, R.Polder, *Corrosion of Steel in Concrete: Prevention, Diagnosis, Repair*, Wiley, (Weinheim, 2004).

5. F. Cui and A. A. Sagüés, “Cathodic Behavior of Stainless Steel 316LN Reinforcing Bars In Simulated Concrete Pore Solutions”, Paper No. 08323, Corrosion/08, (Houston, TX: NACE, 2008).

6. P. Castro, A.A.Sagüés, E.I. Moreno, L. Maldonado and J. Genesca, “Characterization of Activated Titanium Solid Reference Electrodes for Corrosion Testing of Steel in Concrete", Corrosion, Vol. 52 (1996) p.609,

7. “MMFX product bulletin”, MMFX Steel Corporation of America, (2001).

8. A.A. Sagüés, S. Virtanen and P. Schmuki, “Oxygen Reduction on Passive Steel and Cr Rich Alloys for Concrete Reinforcement”, p.p. 305-310 in “Passivation of Metals and Semiconductors, and Properties of Thin Oxide Layers”, Philippe Marcus and Vincent Maurice, Eds., Elsevier, (Amsterdam, 2006).

9. A.A. Sagüés, M..A. Pech-Canul and Shahid Al-Mansur, “Corrosion Macrocell Behavior of Reinforcing Steel in Partially Submerged Concrete Columns”, Corrosion Science, Vol.45 (2003) p. 7-32

10. ASTM C876-91(1999) Standard Test Method for Half-cell Potentials of Uncoated Reinforcing Steel in Concrete, (West Conshohocken, PA: ASTM).

11. R. Myrdal, “Phenomena that Disturb the Measurement of Potentials in Concrete”, Paper No. 0339, Corrosion/1996, (Houston, TX: NACE, 1996).

12. M. Orazem, B. Tribollet, *Electrochemical Impedance Spectroscopy*, Wiley, (New Jersey, 2008), p.95.

13. A.A. Sagüés, S.C. Kranc, and E. Moreno, “Time Domain Response of a Corroding System with Constant Phase Angle Interfacial Component: Application to Steel in Concrete” , Corrosion Science, Vol.37 (1995), p.1097.

14. C. Andrade, M. Keddam, Nóvoa, M. C. Pérezc, C. Rangeld, H. Takenouti, “Electrochemical Behaviour of Steel Rebars in Concrete: Influence of Environmental Factors and Cement Chemistry”, Electrochimica Acta,Vol. 46, Issues 24-25, (2001). p.3905-3912

15. Hakiki, Da Cunha Belo, A. Simoes and M. Ferreira, “Chemical Composition and Electronic Structure of the Oxide Films Formed on 316L Stainless Steel and Nickel Based Alloys in High Temperature Aqueous Environments”, J. Electrochem. Soc., Vol. 145, No.11, (1998). p. 3821-3829

16. Sagüés, A.A., Perez-Duran, H. and Powers, R.G., "Corrosion Performance of Epoxy-Coated Reinforcing Steel in Marine Substructure Service", Corrosion, Vol 47(1991), p.884.

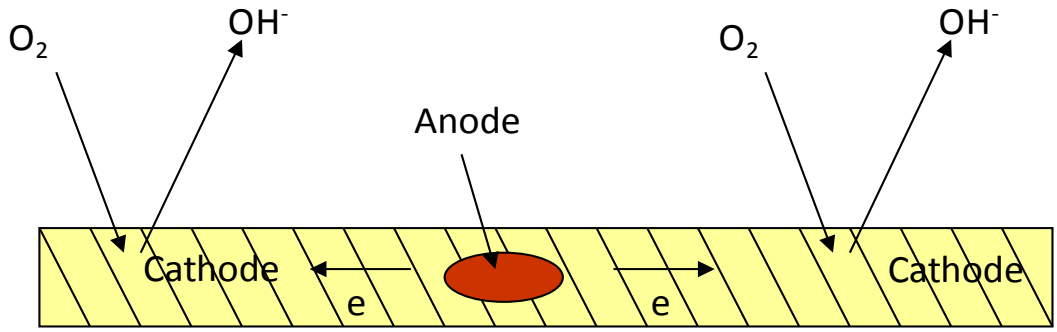

Figure 1: Schematic of cathodic reaction taking place on extended passive surfaces around the active corrosion spot after C_T was exceeded locally.

Figure 2: Appearance of duplicate specimens [from left to right: As-received 9%Cr, Surface blasted 9%Cr, As-received CS, Surface blasted CS].

Table 1
Elemental Composition of 9% Cr (left) and CS (right)
Obtained by Energy Dispersive X-Ray Spectroscopy (C not included)

9% Cr Steel

Element	Wt%
Si	0.24
Cr	0.08
Mn	1.45
Fe	97.48
Cu	0.75

Carbon Steel

Element	Wt%
Si	0.29
Cr	9.09
Mn	0.71
Fe	89.91

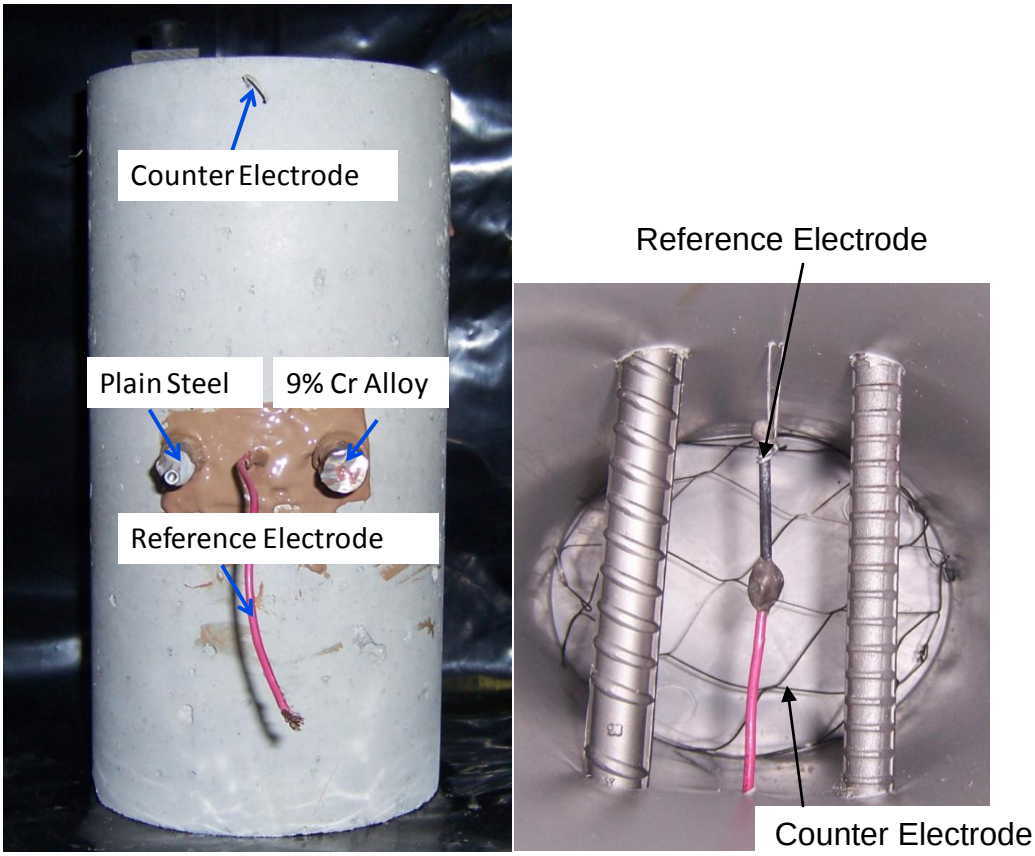

Figure 3: 3-Electrode cell configuration; Bars were centered 6.5 cm apart [Side-view on left, Top-view before casting (surface blasted bars) on right].

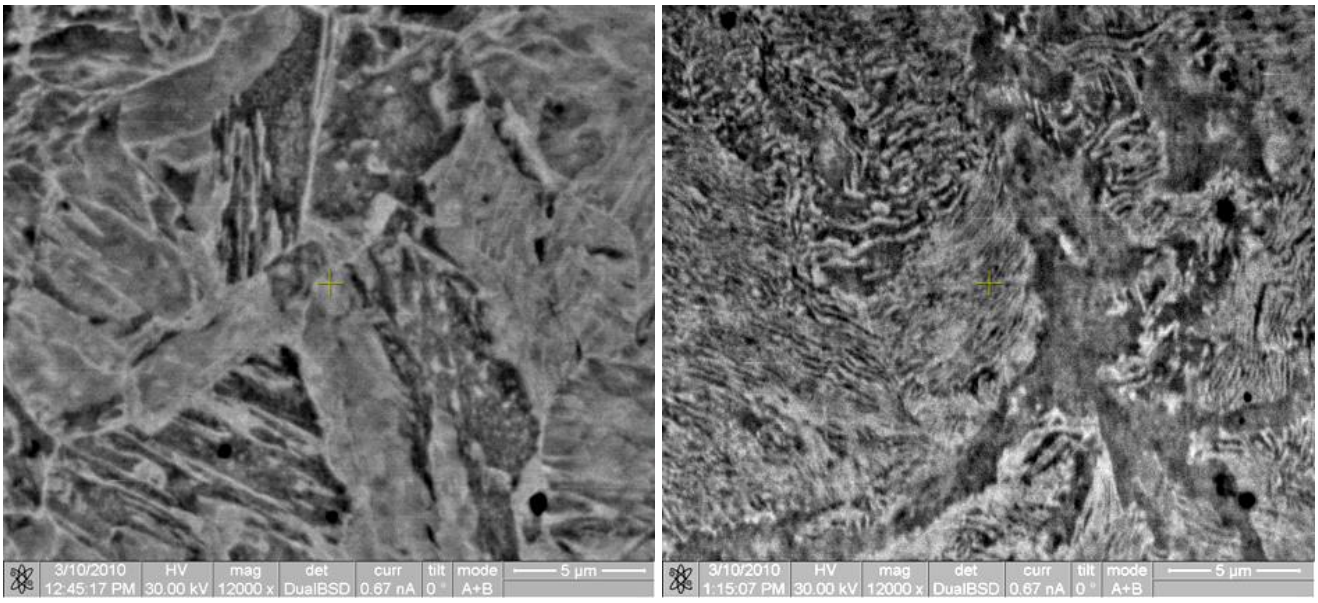

Figure 4: Microstructure of 9% Cr (left) and CS (right) obtained by SEM.

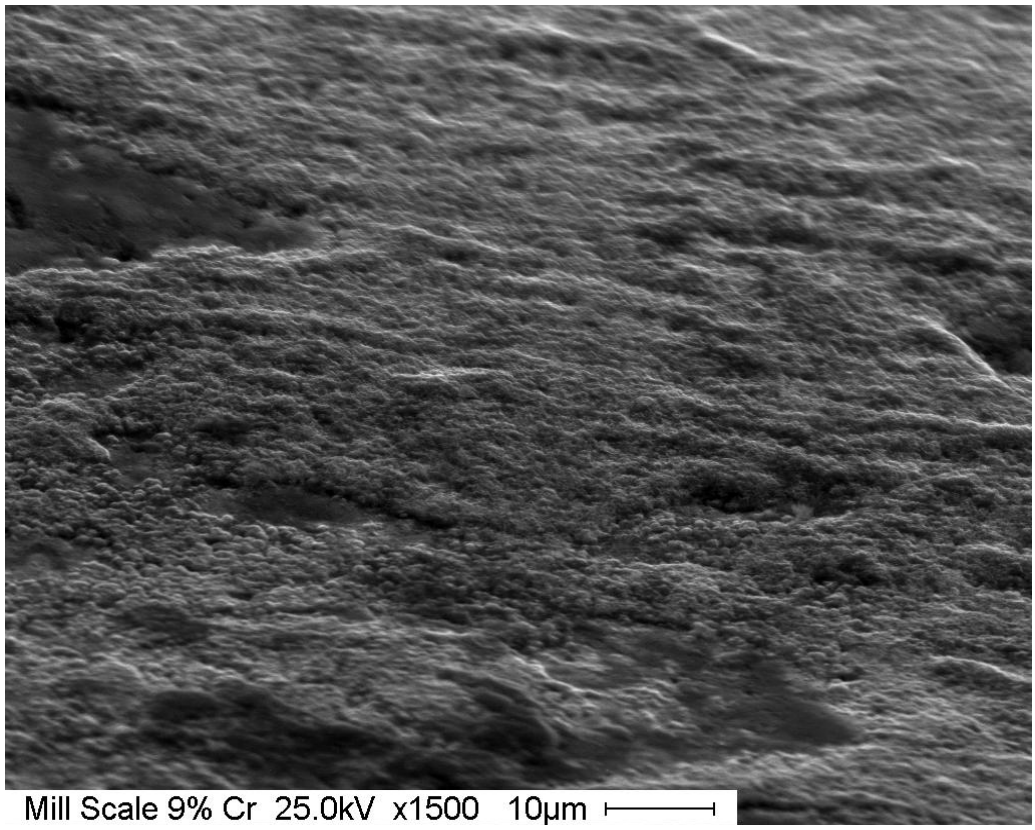

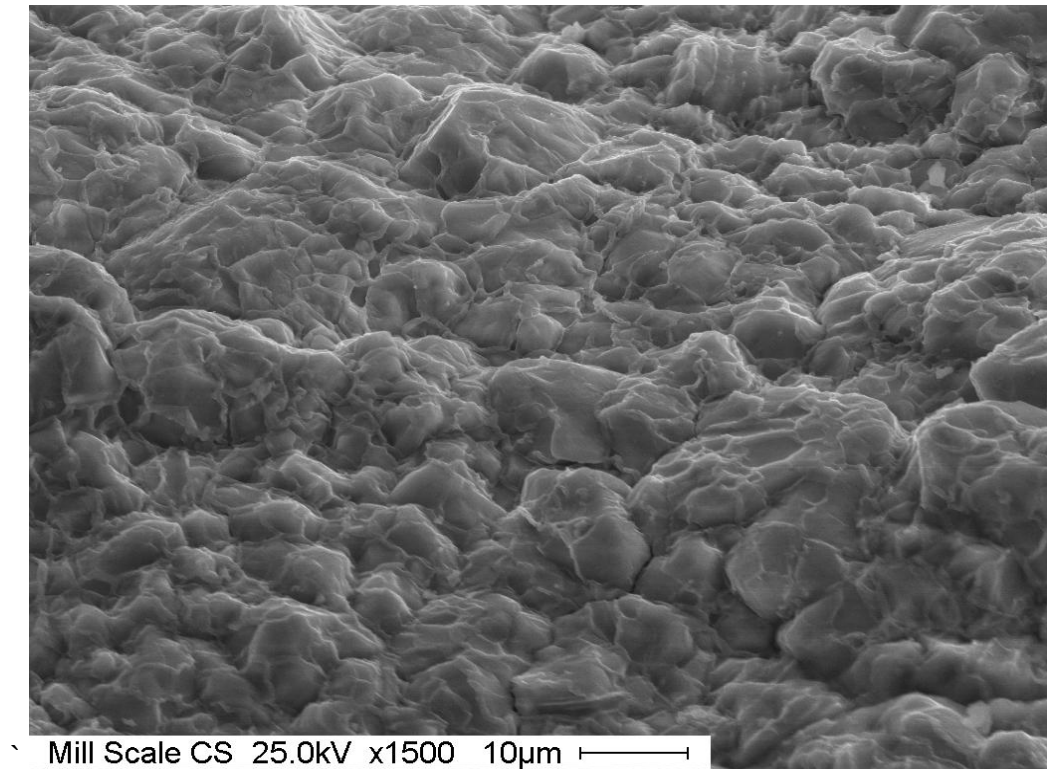

Figure 5: Mill Scale surface of 9% Cr (Top) and CS (Bottom) obtained by SEM.

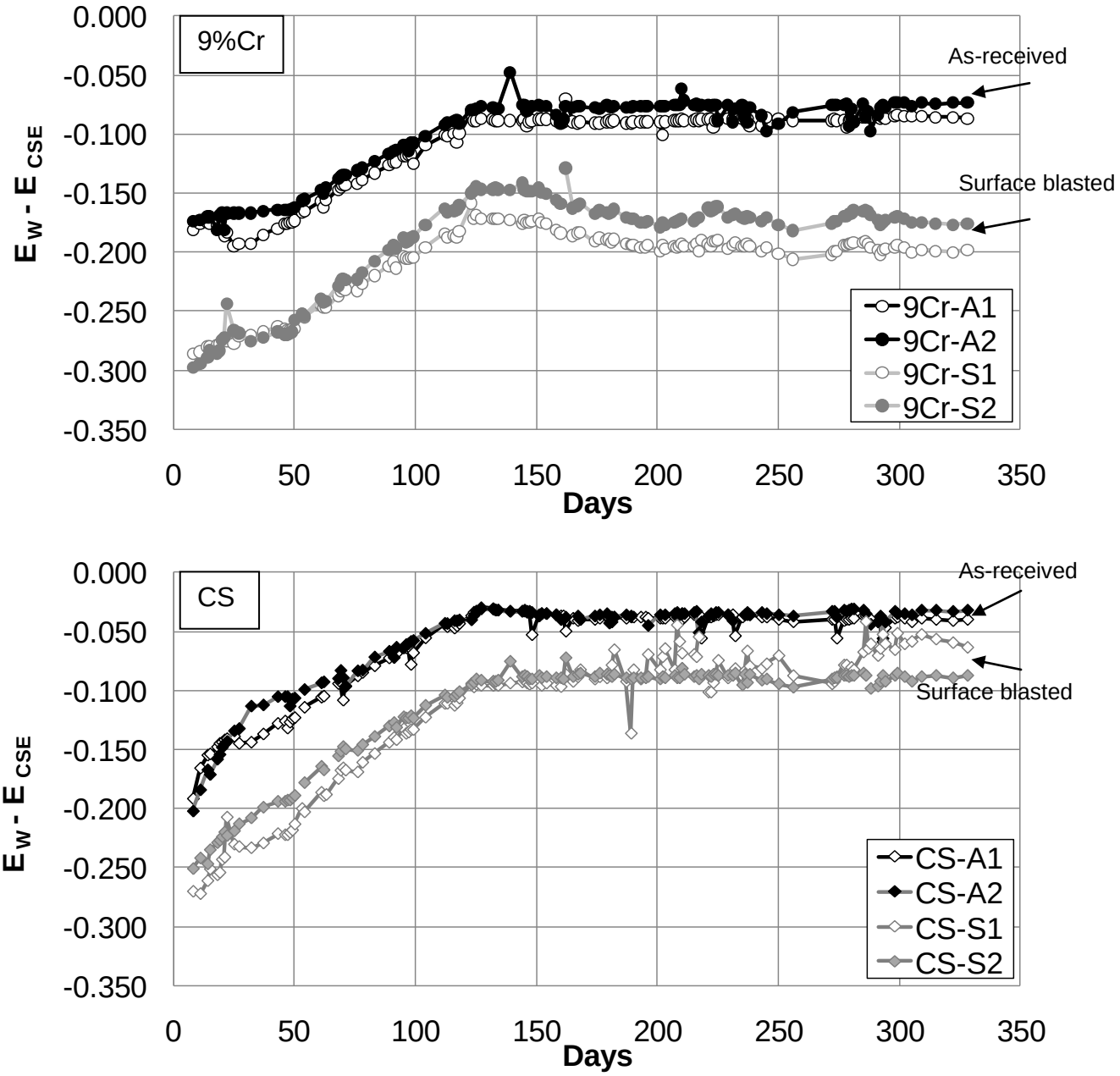

Figure 6: Open circuit potential evolution with time of As-received and Surface blasted rebars [behavior of duplicate specimens; specimen identifiers shown].

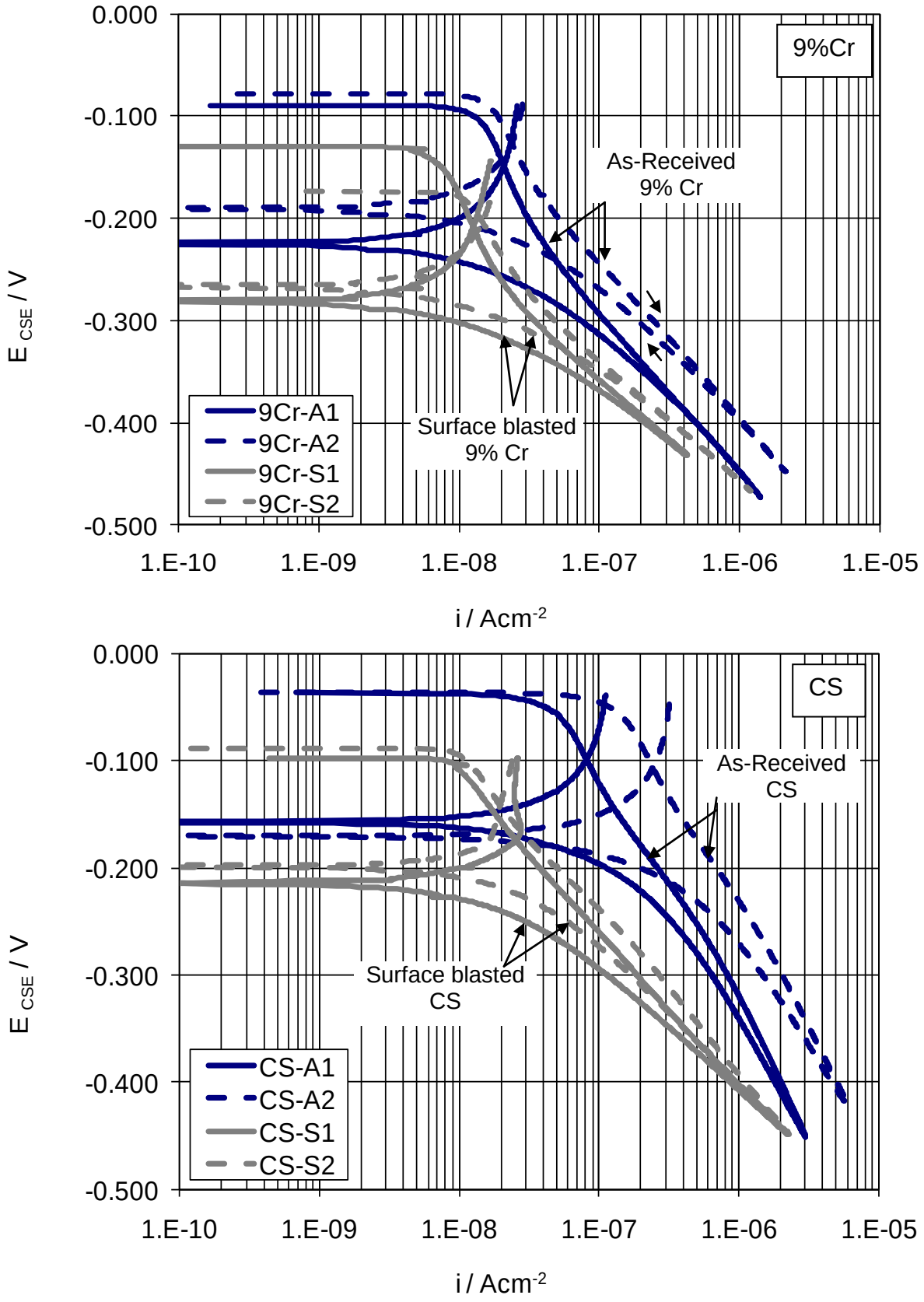

Figure 7: Cathodic polarization graphs of duplicate specimens (specimen identifiers shown) at 191 days. Top, CS; Bottom, 9% Cr. Forward and return directions indicated in the top rightmost graph, similar in the other cases.

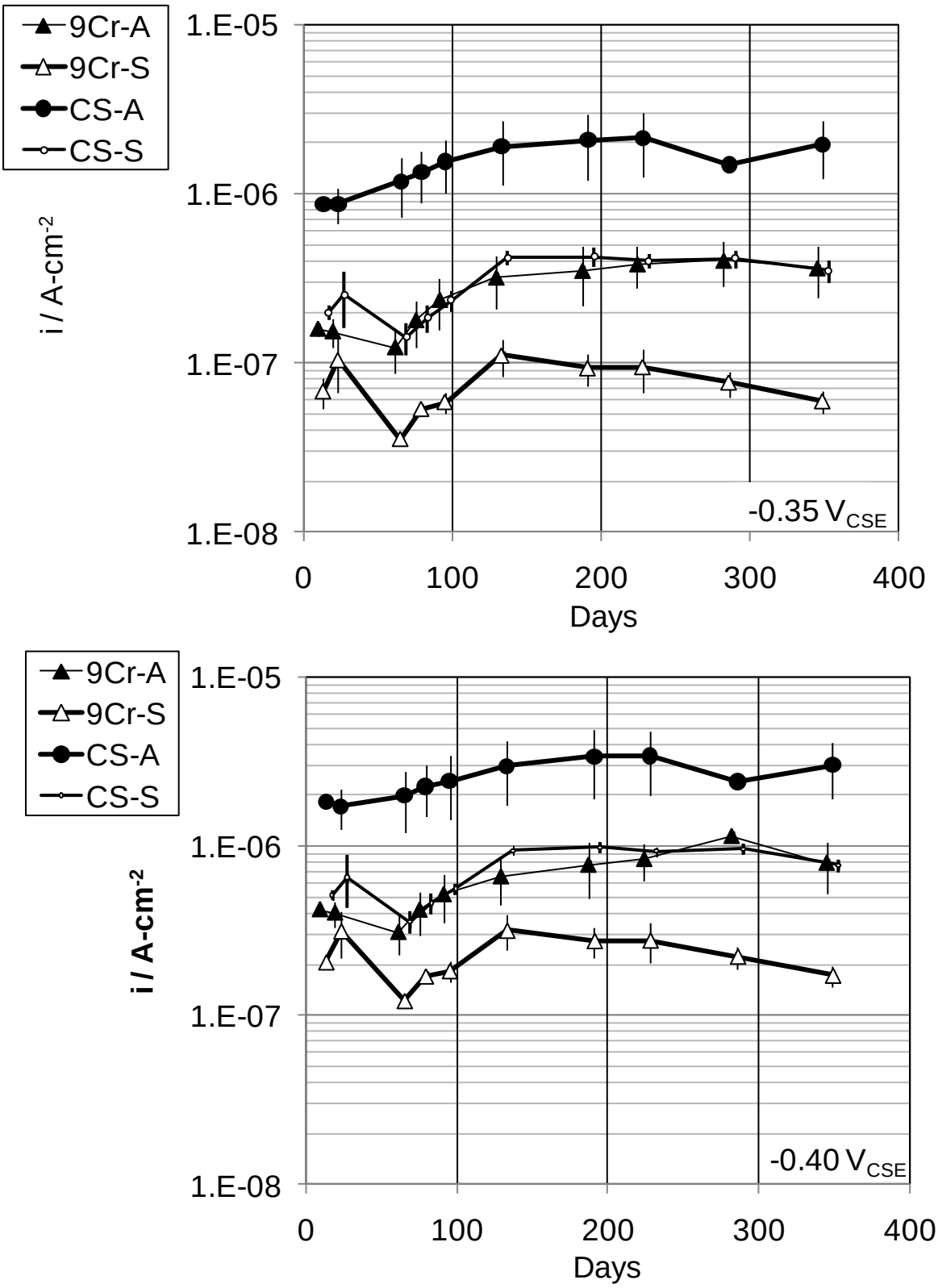

Figure 8: Cathodic polarization current density (i) at -0.35 and -0.40V_{CSE} for all materials and conditions tested. Age in days indicated in each case. Average of duplicate specimens, showing range of values . A and S denote as-received and surface blasted conditions respectively. Single datum only available for CS-A at 280 days.

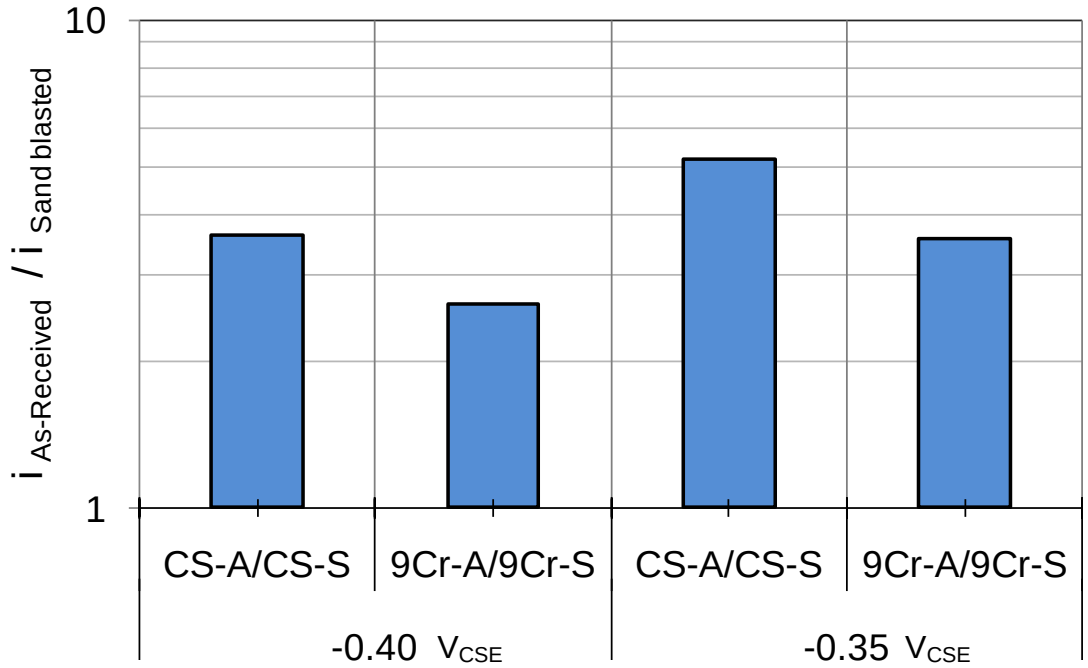

Figure 9: Ratios of cathodic strength of as-received / surface blasted. A and S denote as-received and surface blasted conditions respectively. Average of duplicate specimens for a given material and condition over a one year period.

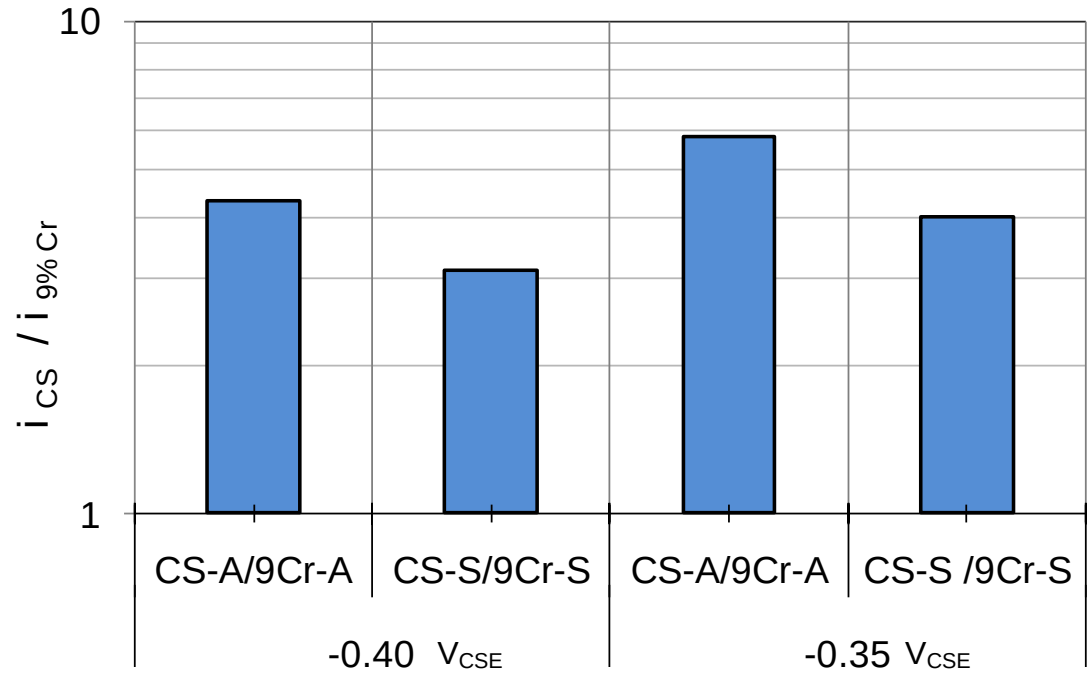

Figure 10: Ratios of cathodic strength of CS / 9% Cr surfaces. A and S denote as-received and surface blasted conditions respectively. Average of duplicate specimens for a given material and condition over a one year period.

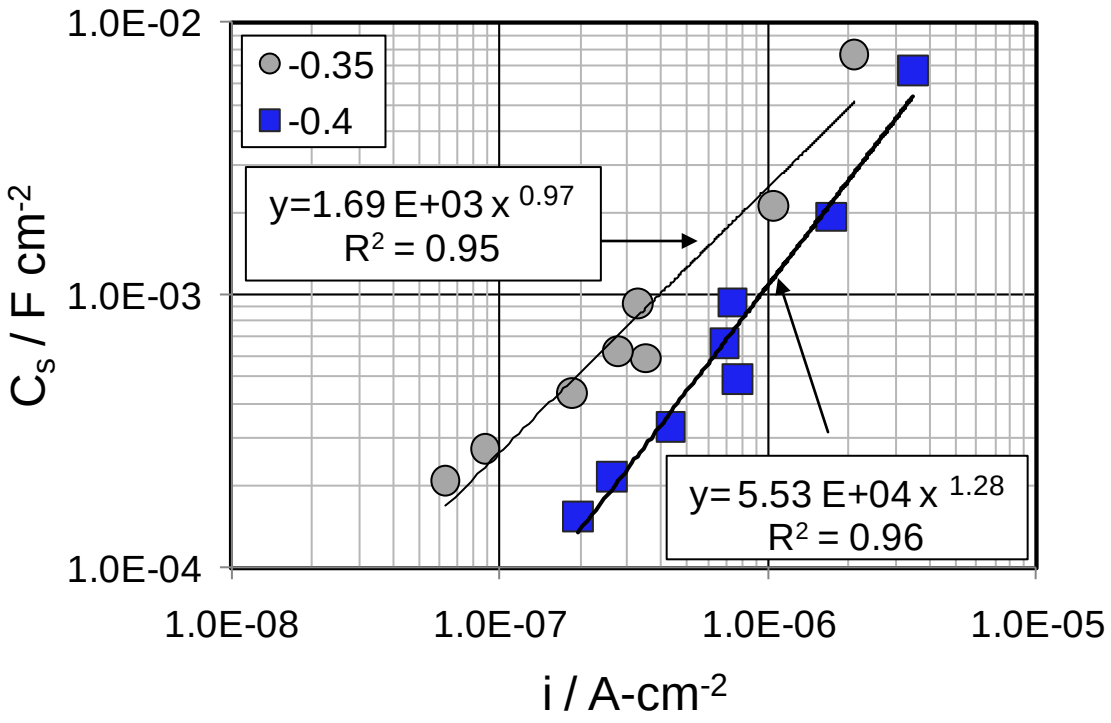

Figure 11: Charge storage parameter as function of cathodic current density i .Composite of all averaged results of duplicate specimens in each condition, at each of the two evaluation potentials. The legend shows the fit parameters and quality for a power-law relationship between both variables.